energies

*Article*

# Agnostic Battery Management System Capacity Estimation for Electric Vehicles

**Lisa Calearo [1,2], Charalampos Ziras [1], Andreas Thingvad [3] and Mattia Marinelli [1,*]**

1 Department of Wind and Energy Systems, Technical University of Denmark (DTU), Risø Campus, 2800 Roskilde, Denmark
2 Ramboll Danmark A/S, 2300 Copenhagen, Denmark
3 Hybrid Greentech ApS, 4000 Roskilde, Denmark
* Correspondence: matm@dtu.dk

**Abstract:** Battery degradation is a main concern for electric vehicle (EV) users, and a reliable capacity estimation is of major importance. Every EV battery management system (BMS) provides a variety of information, including measured current and voltage, and estimated capacity of the battery. However, these estimations are not transparent and are manufacturer-specific, although measurement accuracy is unknown. This article uses extensive measurements from six diverse EVs to compare and assess capacity estimation with three different methods: (1) reading capacity estimation from the BMS through the central area network (CAN)-bus, (2) using an empirical capacity estimation (ECE) method with external current measurements, and (3) using the same method with measurements coming from the BMS. We show that the use of BMS current measurements provides consistent capacity estimation (a difference of approximately 1%) and can circumvent the need for costly experimental equipment and DC chargers. This data can simplify the ECE method only by using an on-board diagnostics port (OBDII) reader and an AC charger, as the car measures the current directly at the battery terminals.

**Keywords:** battery capacity; electric vehicle; DC charger; on-board charger; BMS data



**Citation:** Calearo, L.; Ziras, C.; Thingvad, A.; Marinelli, M. Agnostic Battery Management System Capacity Estimation for Electric Vehicles. *Energies* **2022**, *15*, 9656. https://doi.org/10.3390/en15249656

Academic Editors: Cesar Diaz-Londono and Yang Li

Received: 24 November 2022
Accepted: 15 December 2022
Published: 19 December 2022



## 1. Introduction

### 1.1. Motivation

Due to the rapid growth of electric vehicle (EV) adoption, it is becoming increasingly important to understand how batteries degrade over a vehicle's lifetime. Li-ion battery packs used in EV applications are always equipped with a battery management system (BMS) [1]. This measures, controls, and manages battery usage [2], while keeping the voltage, current, and temperature of the battery in a safe operating area [3]. In addition, a BMS estimates capacity, a metric used to evaluate battery capacity loss. However, capacity estimations are not standardized between car manufacturers, and internal BMS estimations can vary from car to car depending on the applied method, frequency of recalibration, etc. Additionally, a few commercially available solutions have been developed to estimate the capacity of EV batteries, by using charge or discharge processes and relying on the BMS data. However, we are left with the question, Are EV BMS capacity estimations always reliable and accurate?

### 1.2. Capacity Estimation Techniques

BMS estimation techniques are divided into two groups: adaptive and experimental [4]. In adaptive methods capacity is estimated from parameters that are sensitive to the degradation of the battery cell. Examples are neural networks [5] or Kalman filters [6], which can provide accurate results. However, high computational needs and costs limit their application in commercial systems [4]. In experimental methods the cycling data history of the battery is stored, and capacity is estimated as a comparison with previously gained knowledge. The computational effort of experimental methods is lower, simplifying their implementation to the disadvantage of lower accuracy. An example is given when BMS capacity estimations are performed onboard by correlating the ampere hours charged or discharged with the voltage difference [1]. Estimation errors accumulate when ampere-hour counting is performed over a long period of time, resulting in inaccuracies and the need for recalibration. Nevertheless, thanks to its simplicity, the combination of Coulomb counting and state-of-charge (SOC)–open circuit voltage relation is used in current BMSs.

Hybrid adaptive/experimental methods, which first characterize chemical reactions and aging mechanisms are also proposed. They are based on approaches such as incremental capacity analysis (ICA) and differential voltage analysis [7], which have been mainly used as reliable offline tools, and have been investigated for online BMS applications [7]. The ICA method relies on plotting the derivative of the capacity with respect to voltage as a function of voltage (incremental capacity (IC) signature) [8,9]. As the battery experiences degradation, the peaks of the IC signature change location. Peaks and valleys of an aged battery can then be compared to the ones of a new battery, and thereby derive the capacity of the aged one [10]. This method has been applied at the EV level in [10,11], showing comparable characteristic peaks and valleys of the IC signature between cells and pack. However, the authors of [12,13] claim that the pack signature may not be directly extrapolated from the already available cells, given that those are not always subject to similar conditions.

Given the wide range of commercially available BMSs and the lack of transparency, it is important to be able to estimate battery capacity with a methodology that is agnostic to BMS data processing and can be applied on any EV battery chemistry, size, and usage. A methodology with such potential is an empirical capacity estimation (ECE) method, used for the first time in our previous work [14], but only applied to a 24 kWh Nissan Leaf. The method consists of a full charge of the battery without disassembling it from the vehicle and violating the warranty. When charging with onboard (AC) chargers, battery voltage and current are not accessible for measurement due to the presence of the AC/DC converter. Therefore, an external DC charger is used, where charging voltage and current can be measured with external equipment at the DC charger terminals. Capacity is then determined as the energy flowing into the battery during the full charge. The disadvantage of this method is that it is time consuming and requires the use of external equipment (EE) that is expensive and not readily accessible.

### *1.3. What Data Is Available*

In series-produced cars, valuable BMS data can be read from the central area network (CAN)-bus via the on-board diagnostics port (OBDII). Available data includes instantaneous measurements, like battery voltage and current, and BMS-derived battery capacity estimations. On the one hand, this allows the use of BMS voltage/current measurements in the ECE method instead of that from EE, after first evaluating their accuracy. On the other hand, BMS estimations can be evaluated and compared with values obtained through a BMS-agnostic method.

The three levels of data which are considered in this work are displayed in Figure 1. They are

- voltage and current measured with EE during a full charge (in green), used to estimate capacity with the ECE method;
- voltage and current BMS measurements read through the OBDII port (in blue), used to estimate capacity with the ECE method; and
- capacity readings from the CAN-bus (in red), which are internally estimated by the BMS, the exact estimation process of which is unknown to the authors.

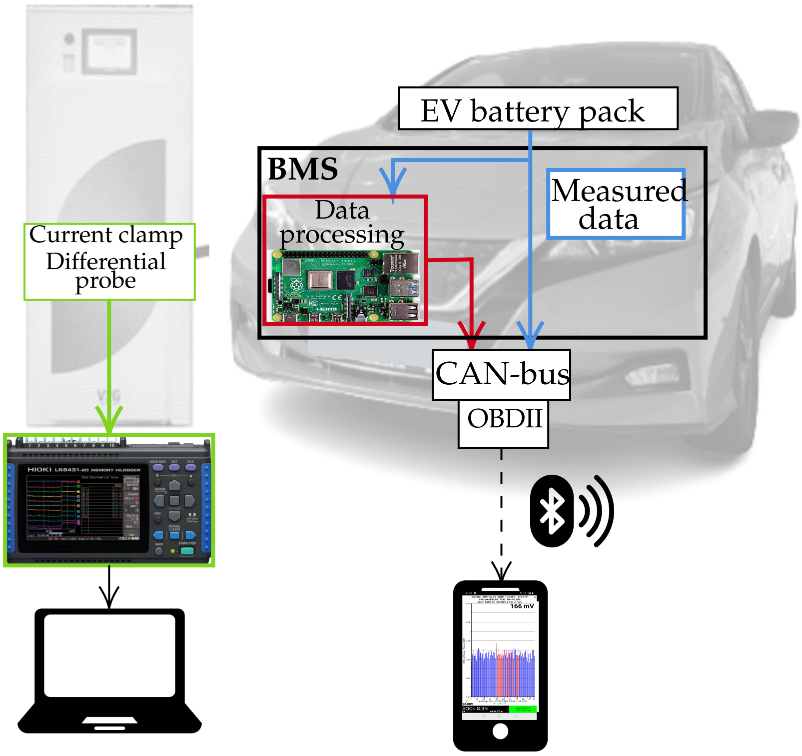


**Figure 1.** Data collection overview. On the left, current and voltage measurements are collected from the DC charger with current clamp, differential probe, and datalogger. On the right, raw measurements (in blue) are collected from the BMS and CAN-bus, together with estimations derived by the EV microcomputer.

### 1.4. Paper Contributions

In this work, we investigate and compare three capacity estimation approaches for six different EV batteries, without disassembling them from the vehicles. The main objective is to assess whether BMS readings can be used to circumvent the need for costly and invasive experimental measurements.

The main contributions can be summarized as follows.

- First, capacity readings from the CAN-bus are compared with estimations from the ECE method, while providing insight regarding the observed differences.
- Secondly, the validity of BMS instantaneous current and voltage measurements is assessed by comparing them with EE measurements.
- Thirdly, EE and BMS current/voltage datasets are used to estimate battery capacity with the ECE method, and a comparison between the two is provided.

### 1.5. Paper Organization

The rest of the paper is structured as follows. Section 2 presents the theoretical background for the capacity derivation. Section 3 presents the measurement methodology for the estimation of EV battery capacity. Section 4 overviews the case study, along with battery pack information and vehicle usage characteristics. Section 5 compares the battery capacity estimations with the different datasets. Section 6 concludes the manuscript with the main outcomes.

## 2. Theoretical Background

### 2.1. EV Battery Capacity

The total capacity of a battery ($Q$) is the amount of energy the pack can hold. This is a function of the initial energy capacity ($Q_{\mathrm{i}}$), and it decreases over time due to irreversible degradation mechanisms, calendar, and cycle aging. $Q_\mathrm{i}$ represents the amount of energy that the battery can theoretically hold when it is new. The total battery capacity at time $t$ is expressed as

$$Q(t) = Q_\mathrm{i}(1 - (q_\mathrm{cal}(t) + q_\mathrm{cycle}(t))). \tag{1}$$

$q_\mathrm{cal}$ and $q_\mathrm{cycle}$ are the accumulated calendar and cycle degradation, respectively, expressed as a percentage of $Q_\mathrm{i}$. Calendar aging is a function of time, temperature, and SOC, and occurs even when the battery is not used. Cycle aging is a function of the active usage, in terms of full equivalent charge cycles at a certain temperature and current C-rate [14,15]. To maintain the battery lifespan of EVs, BMSs can restrict capacity usage by introducing energy reserves [16]. Thus, EV battery pack capacity can be distinguished between total and usable. Total capacity is the amount of energy the pack can hold without accounting for external restrictions. Usable capacity is the amount of energy that can be stored in the pack, limited by the BMS to protect the battery. If there is no reserve, then the usable capacity coincides with the total capacity. Moreover, it is important to point out that capacity depends on the test conditions and cannot be defined irrespective of them. Indeed, battery capacity changes with different temperatures and C-rate, and the test conditions are not standardized [17].

### *2.2. ECE Method*

The usable energy capacity of a battery can be derived based on the ampere-hour exchange, or the energy exchange during a full charge or discharge cycle. Capacity in Ah is used for the vehicle internal capacity estimation, whereas capacity in Wh is usually provided as nameplate rating by EV manufacturers. Therefore, in this article, we consider both definitions.

Without disassembling the battery from the EV, the usable capacity can be measured during a full EV battery pack charging, and this corresponds to the total capacity if there are no reserves. In Ah ($Q^\mathrm{Ah}$), capacity can be derived by integrating the current $I(k)$ during the full charge. With a time resolution of $\tau = 1\,\mathrm{s}$, $\Delta\mathrm{T} = 3600\,\mathrm{s/h}$ and $\mathrm{N^s}$ being the number of seconds on the full charge, $\mathrm{Q^{Ah}}$ is derived as

$$Q^\mathrm{Ah} = \frac{1}{\Delta\mathrm{T}} \sum_{k=1}^{\mathrm{N^s}} I(k)\tau. \tag{2}$$

Notice that time index $t$ is dropped in $\mathrm{Q^{Ah}}$ and subsequent capacity values to simplify notation. These values will refer to the time when an experiment to estimate capacity was conducted.

When considering the battery capacity in Wh, the charging capacity accounts also for the heat dissipation in the battery internal resistance [14]. If charging is conducted with a low current C-rate, the heat dissipation should be limited and influence the results by a few percentage points. The capacity in Wh ($Q^\mathrm{Wh}$) is derived by integrating the product between the pack voltage $V(k)$ and current $I(k)$ as

$$Q^\mathrm{Wh} = \frac{1}{\Delta\mathrm{T}} \sum_{k=1}^{\mathrm{N^s}} I(k)V(k)\tau. \tag{3}$$

## 3. Measurements Methodology

The battery needs to be fully discharged and then fully charged to measure its capacity. The measurable capacity, without disassembling the battery from the EV and violating the warranty, is the usable capacity, which coincides with the total if no reserve is present. This section presents the system—EV and charger—used for conducting the measurements in Section 3.1, the collected datasets in Section 3.2, and finally the methodology for performing the tests in Section 3.3.

### *3.1. System Layout*

EVs can be charged via DC or AC chargers. When using an AC charger, power is first converted from the AC/DC onboard charger in the vehicle, and then flows into the Li-ion EV battery, see Figure 2. By using a DC charger, the power-dependent losses of the AC/DC on-board charger are avoided. The DC charger directly injects power into the 400 V bus, as shown in Figure 2. While charging, the motor side is off and no power is absorbed. Therefore, the power going to the 400 V bus is shared between the Li-ion EV battery and the 12 V bus supplying the auxiliary systems.

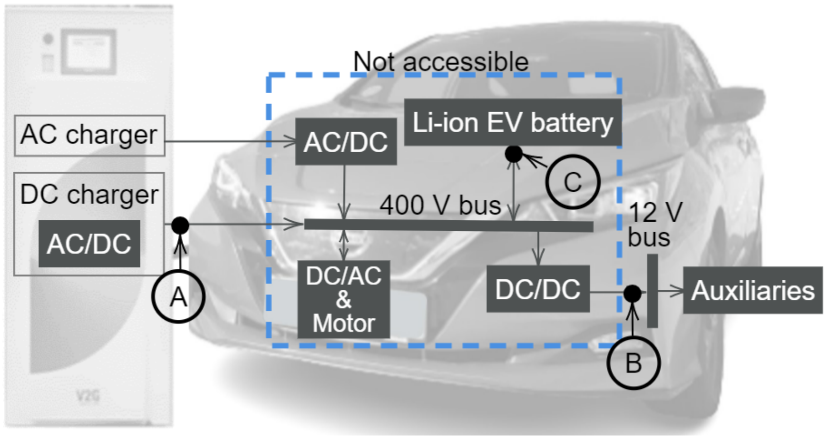


**Figure 2.** Overview of EV power flows. Modified from [14].

### *3.2. Data Collection*

As shown in Figure 1, three types of data are available to determine EV battery capacity with three different estimation methods.

#### 3.2.1. EE Data

This dataset consists of the voltage and current measured at the DC side of the charger (point A) and at the 12 V bus (point B) (see Figure 2). Current and voltage values are collected by using EE: current clamps for the former and voltage differential probes for the latter, with an overall measurement accuracy of 2.3% [14]. Measurements and estimated capacity are referred to as EE data.

#### 3.2.2. BMS Data

This dataset consists of the voltage and current measured on point C in Figure 2 from the BMS of the vehicle. This data is collected with a maximum resolution of one value per second. It is read through the CAN-bus and OBDII port by using the Nissan Leaf Spy app [18], and becomes available to the user in a spreadsheet form. The accuracy of the EV internal measurement equipment is unknown to the authors and will be further investigated in this article. These measurements are referred to as BMS data.

#### 3.2.3. CAN-Bus Data

The last dataset consists of battery capacity readings from the CAN-bus OBDII port. These values are internally estimated by the vehicle. The estimated capacity values are referred in the following as CAN-bus readings.

### *3.3. Measurement Process*

EV battery pack capacity is measured with the ECE method, which is explained and extended in this section. The method is applicable for all car brands that can be charged with DC power via an external charger [14].

The ECE method involves a full charge of the battery pack from the minimum to the maximum SOC. The charging process consists of two phases. The first is constant current, in which the current is kept constant until voltage reaches the maximum value. The second is constant voltage, where battery voltage is at its maximum value, and current decreases until the charger stops charging. During the measurements it was observed that DC chargers stop charging when the current drops to approx. 3 A. This limitation was experienced with four chargers of two different brands and all investigated vehicles. This behaviour is assumed to be a common feature of DC charging due to the unnecessarily long charging time with very low efficiency. After the DC charger stops, the battery can still be charged if connected to an AC charger (see Figure 3). The amount of energy depends on the minimum current reached by the DC charger. The higher the minimum current, the higher the energy that can be charged with the AC charger.

If the battery pack is small, this energy can be a significant share of the total capacity. Therefore, the methodology in [14] has been revised in this work as follows. After the DC charger stops, the charging process is complemented with the final tail obtained by connecting an AC charger (AC charging tail). Two such examples are provided in Figure 3. Differently from the DC charger, the power coming from the AC charger goes through the AC/DC inverter and then to the Li-ion EV battery (see Figure 2). Measuring the current at the AC side would account for the inverter losses; therefore, this is avoided by considering the current measured at the terminals of the battery (point C in Figure 2). Without disassembling the battery, these values can only be obtained by the BMS.

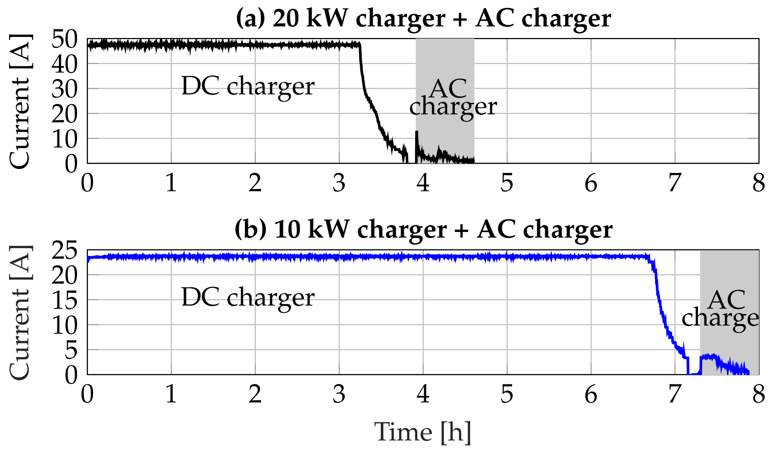


**Figure 3.** Current charging profiles of a 62 kWh battery pack with a 10 kW and a 20 kW DC charger, including the final tail with an AC charger.

Battery capacity can be derived by considering the current and voltage measured during the charging period with the two datasets (EE and BMS). Figure 4 shows the respective measurement locations. Voltage and current read from the BMS are internally measured at the battery terminals in point C, whereas EE data is measured at the DC charger side (point A) and at the 12 V bus (point B). To compare voltage and current, EE data are processed to derive the current at the battery terminals. This is calculated as the difference between the current in points A and B*. To derive the current in B* ($I^{\mathrm{B}^*}(k)$), the current in B is scaled to the 400 V bus by considering the voltage measured in A (400 V bus, $V^{\mathrm{A}}(k)$) and B (12 V bus, $V^{\mathrm{B}}(k)$) as in (4):

$$I^{\mathrm{B}^*}(k) = I^{\mathrm{B}}(k) \cdot \frac{V^{\mathrm{B}}(k)}{V^{\mathrm{A}}(k)}. \tag{4}$$

DC/DC converter losses between the 400 V and 12 V buses are assumed to be negligible.

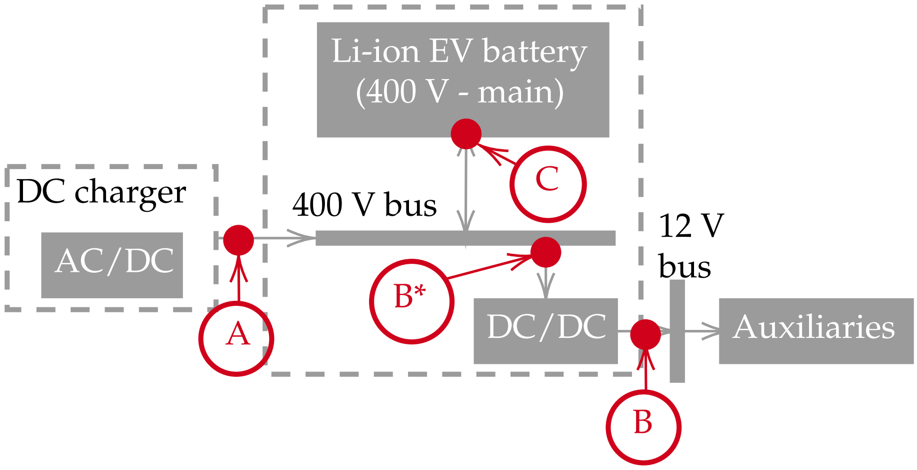


**Figure 4.** Measurement location overview. In A and B, voltage and current are measured with the external equipment. The BMS voltage and current data are measured from point C. B* is the derived current measurement with the external equipment.

By using (2), capacity is derived by (5) considering the external measurements in points A and B and the additional AC tail, and by (6) considering the BMS current measurements in point C:

$$Q_{\mathrm{EE}}^{\mathrm{Ah}} = \frac{1}{\Delta \mathrm{T}} \left( \sum_{k=1}^{\mathrm{N}_{\mathrm{DC}}^{\mathrm{s}}} \left( I^{\mathrm{A}}(k) - I^{\mathrm{B}^*}(k) \right) \tau + \sum_{k=\mathrm{N}_{\mathrm{DC}}^{\mathrm{s}}+1}^{\mathrm{N}_{\mathrm{DC}}^{\mathrm{s}}+\mathrm{N}_{\mathrm{AC}}^{\mathrm{s}}} I^{\mathrm{C}}(k)\tau \right), \tag{5}$$

$$Q_{\mathrm{BMS}}^{\mathrm{Ah}} = \frac{1}{\Delta \mathrm{T}} \sum_{k=1}^{\mathrm{N}_{\mathrm{DC}}^{\mathrm{s}}+\mathrm{N}_{\mathrm{AC}}^{\mathrm{s}}} I^{\mathrm{C}}(k)\tau, \tag{6}$$

where $\mathrm{N}_{\mathrm{DC}}^{\mathrm{s}}$ and $\mathrm{N}_{\mathrm{AC}}^{\mathrm{s}}$ is the number of seconds while charging with the DC and AC charger, respectively. Similarly, battery capacity can be derived in Wh by adapting (3).

In the following sections, the normalized capacity $q$ (ratio between the measured and the initial energy capacity) will be used. The superscript Ah or Wh will denote the convention used to express capacity, and the subscript will refer to the used dataset (EE, BMS or CAN).

## 4. Case Study

### *4.1. Battery Characteristics*

Six EVs with different battery size, chemistry, and usage have been chosen, to demonstrate that results are applicable independently of these factors. Additionally, to account for the rapid technology development during the last decade, EVs introduced in 2014 and 2020 are considered. The EVs names and their characteristics are provided in Table 1.

The Ah nominal capacity ($Q_{\mathrm{i}}$) of the EVs can be read through the BMS and Leaf Spy app [18]. Nominal voltage is derived as the average open-circuit voltage measured during the constant current phase of the full charge. To the authors' knowledge, the chemistry of the 30 kWh is still unknown in the literature; however, it is expected to be similar to previous and newer battery versions.

**Table 1.** Vehicles' battery pack and cell characteristics. The number next to E and L indicates the nominal capacity in kWh.

| EVs | Env-200 24 kWh | Env-200 24 kWh | LEAF 30 kWh | LEAF 30 kWh | LEAF 40 kWh | LEAF 62 kWh |
|---|---|---|---|---|---|---|
| **Name** | **E24-1** | **E24-2** | **L30-1** | **L30-2** | **L40** | **L62** |
| Chemistry | LMO [19] | | LMO + NMC(?) | | NMC [19] | NMC [19] |
| Voltage [V] | 369.6 | | 360.0 | | 350.4 | 350.4 |
| Number of cells | 192 | | 192 | | 192 | 288 |
| Cells in series | 96 | | 96 | | 96 | 96 |
| Cells in parallel | 2 | | 2 | | 2 | 3 |
| Capacity [Ah] | 65.4 | | 79.5 | | 115.4 | 176.4 |
| Capacity [kWh] | 24.2 | | 28.6 | | 40.4 | 61.8 |

### *4.2. Vehicle Daily Usage*

All four E24 and L30 vehicles are driven during the day by the local municipality of the Danish island of Bornholm, and provide frequency regulation (FR) during the night since the end of 2016 [20]. Frequency control is provided for approximately 14 h during the weekdays, and during the weekends for the entire day. An external ±10 kW vehicle-to-grid (V2G) charger with CHAdeMO connector is used to provide FR. L40 is parked in the laboratory of the Technical University of Denmark, and is only used for measurements a few times per year [15]. L62 is privately owned and driven daily in Denmark [21]. Usage characteristics are summarized in Table 2. EV battery production date is not provided to the owners; therefore, it is here considered to be two months prior to the registration date. Only for L40 is the battery production set eight months prior because the vehicle was previously used for exhibition purposes [15]. The energy throughput for the distance driven per day is derived considering an average consumption of 6 km/kWh [22]. The energy throughput for the FR service of all four E24 and L30 vehicles is considered as in [14], because the service is based on the same frequency and control strategy.

**Table 2.** Average vehicles usage, distance driven, and FR throughput. * The vehicle provided FR only during the first year.

| EV | E24-1 | E24-2 | L30-1 | L30-2 | L40 | L62 |
|---|---|---|---|---|---|---|
| Registration date | 7 July 2016 | 23 June 2017 | 21 September 2017 | 6 December 2016 | 1 August 2018 | 30 November 2020 |
| Distance per day [km/day] | 10 | 21 | 20 | 21 | 0 | 35 |
| Throughput drive [kWh/day] | 3.3 | 7 | 6.6 | 7 | 0 | 11.7 |
| FR | Yes | No * | Yes | Yes | No | No |
| Throughput FR [kWh/day] | 45 | 45 | 45 | 45 | 0 | 0 |
| Tot. throughput [kWh/day] | 48.3 | 52 | 51.6 | 52 | 0 | 11.7 |
| Active cooling | Yes | Yes | No | No | No | No |

### *4.3. Charging C-Rate*

External 10 kW DC chargers with CHAdeMO connector are used for charging the EV batteries. During the constant current phase, the current is approximately 24 A. For the considered vehicles, this corresponds to a C-rate (defined as the current divided by the nominal capacity in Ah) between 0.37 for the smallest battery and 0.14 for the largest one, see Table 3. In both cases, C-rate should be sufficiently low to keep the battery heat dissipation limited to a few percentage units and estimate the battery capacity [14].

**Table 3.** Current and C-rate during the constant current phase of the charging process.

| EV | E24-1 | E24-2 | L30-1 | L30-2 | L40 | L62 |
|---|---|---|---|---|---|---|
| Capacity [Ah] | 65.4 | | 79.5 | | 115.4 | 176.4 |
| Current [A] | 24 | | 24 | | 24 | 24 |
| C-rate [-] | 0.37 | | 0.30 | | 0.21 | 0.14 |

## 5. Results

Results are presented in three main steps, as shows in Table 4. During the first step (Section 5.1), capacity estimations over five years derived via testing with ECE method and EE data, and readings from the CAN-bus are compared. This step shows the uncertainties arising from the nontransparent BMS estimations. Thus, in the second step (Section 5.2), the instantaneous current and voltage values provided by the BMS are compared with those from EE. These values are then used in the last step (Section 5.3) to compare the capacity estimated with the two datasets, i.e., EE and BMS. Finally, Section 5.4 concludes the section with field test insights on capacity estimation methods and data collection.

**Table 4.** Steps for results comparison.

| | | | |
|---|---|---|---|
| STEP 1: | EE capacity estimate ($q_{EE}$) | VS | CAN-bus capacity estimate ($q_{CAN}$) |
| STEP 2: | EE current and voltage data | VS | BMS current and voltage data |
| STEP 3: | EE capacity estimate ($q_{EE}$) | VS | BMS capacity estimate ($q_{BMS}$) |

### *5.1. Step 1: EE and CAN-Bus Readings Capacity Comparison*

#### 5.1.1. Capacity EE Estimation

Figure 5 compares the normalized capacity of the different vehicles versus their age, both in Ah and Wh. As discussed in Section 3.3, DC chargers stop charging at low current values and more energy can still flow to the battery via AC charging. Despite the fact that this energy is limited for newer and larger batteries, it is important to consider this effect in the overall capacity estimation. A more detailed explanation is provided in Appendix A.2.

The used initial battery capacity values in Ah and Wh are provided in Table 1 and used in this section for normalizing the measured capacity values. By comparing the normalized capacity ($q_{EE}^{Ah}$ and $q_{EE}^{Wh}$) versus age, the different battery chemistry and size do not seem to have a large impact on the degradation trend. L40 ages more slowly, which can be explained by the sole existence of calendar aging, constant battery temperature of 22 °C, and SOC of 50% [15]. Another interesting finding is that kWh capacity values are 3–4% higher than the Ah values. The difference is caused by the battery joule losses that depend on the C-rate during charging. For example, taking a vehicle with battery resistance in p.u. as 6%, if charged with 1 C-rate losses are 6%, whereas if charged with 0.2 C-rate, losses are approximately 1.2%. Therefore, the smaller the battery, the larger the C-rate and the joule losses, and the difference between Ah and Wh normalized values.

Based on Figure 5 the measured capacity does not present a smooth, or even monotonous, decrease. This can be due to different factors. First, battery temperature varied during testing. Despite the fact that measurements were conducted in spring and autumn with similar ambient temperatures, it is not possible to keep the temperature of the batteries constant. Battery temperature variations during the charging phase are kept below 8 °C for most of the cases, with temperatures ranging between 15 °C and 25 °C (see Appendix A.1). Only twice were the battery temperatures of E24-1 and L40 approximately 35 °C, due to usage before the measurements.

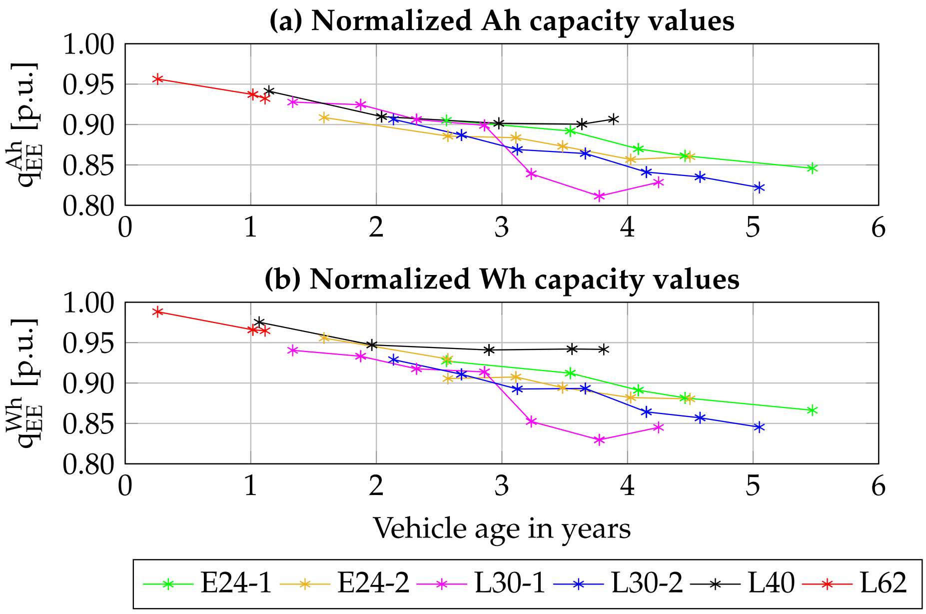


**Figure 5.** Normalized capacity measurements versus age of the vehicles in years.

Secondly, the ±1% accuracy of current and ±0.1% accuracy of voltage measurements are propagated in the final capacity with an accuracy of 2.3% [14]. Thirdly, for what concerns the discharging process, the reached minimum voltage is not always the same, and it does not always correspond to the same minimum SOC (see Table A1). This is because during the discharging phase the BMS stops the discharging process when the lowest cell voltage reaches a level between 2.8 and 3.1 V. Thus, the minimum voltage can differ from test to test, due to a different cell imbalance each time. Nevertheless, because voltage increases quickly in the beginning of the tests (due to the initial steep relationship between SOC and open circuit voltage of Li-ion batteries), the difference of the minimum pack voltage has a limited effect on the measured battery capacity [14].

#### 5.1.2. Comparison of EE and CAN-Bus Readings

Figure 6 compares the normalized measured capacity via the ECE method and EE data ($q_{EE}^{Ah}$) with those collected via the CAN-bus readings ($q_{CAN}^{Ah}$). Because vehicle internal estimations are usually based on Ah values, this section is only focused on those.

CAN-bus capacity readings are always higher than the measured ones, with the exception of L30[2]. Moreover, CAN-bus readings above the initial capacity value (larger than 1 p.u.) are observed for E24-1 and E24-2, whereas L30-1 dropped from 0.78 p.u. to 0.69 p.u. in less than 6 months. For older vehicles, E24 and L30, larger differences between the EE measurements and CAN-bus readings are observed. The CAN-bus capacity readings cannot be fully explained by the authors, because they depend on internal vehicle estimation.

Furthermore, the computing power, available memory and accuracy of the current measurements can impact capacity estimations [1]. Although it is not possible to assess the first two (and the method used by the EV microcomputer), current and voltage measurements at the battery terminals can be collected from the BMS through the OBDII. Therefore, in the next subsection the accuracy of voltage and current measurements is investigated by comparing them with EE values.

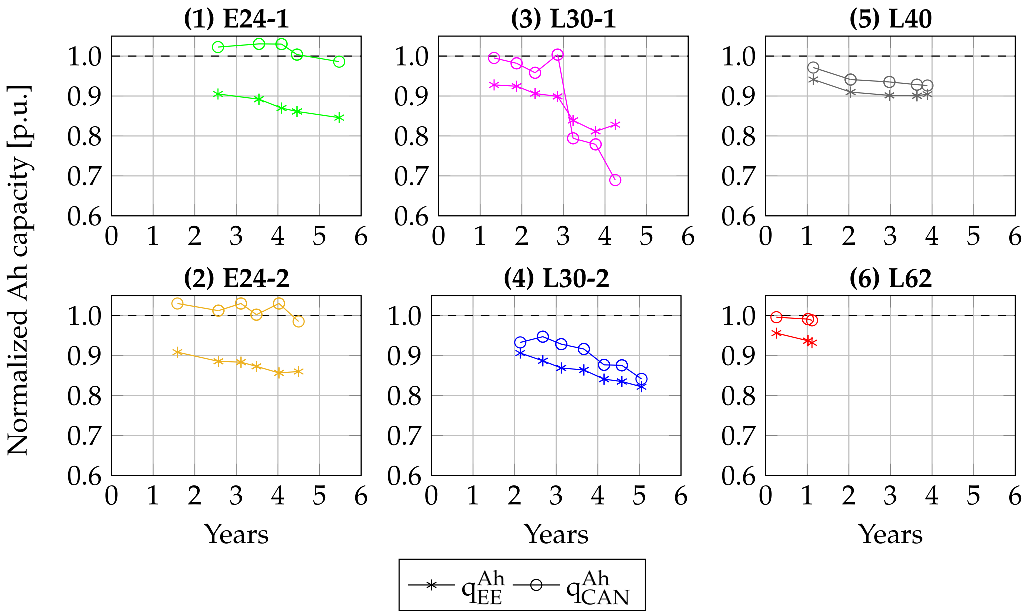


**Figure 6.** Normalized Ah capacity comparison between the measured EE (represented by asterisks) and CAN-bus readings (represented by circles).

### 5.2. Step 2: EE and BMS Current and Voltage Comparison

In this subsection, the accuracy of the battery voltage and current BMS measurements is investigated. This is done by comparing the values measured from the BMS with those measured by the EE dataset. As shown in Figure 4, the EE current at the battery terminal (point B*) is derived from the EE measurements in A and B considering (4). Measurements are compared in terms of the instantaneous percentage difference in Figure 7 during the first charging hour of the measurements. Table 5 provides the standard deviation (SD) and mean values of the percentage difference of the current and voltage values during the constant current phase of the charging process.

Subplot (a) shows that the voltage difference is always limited to ±0.5%, whereas in (b) the current difference varies between ±8% for E24 and L30, and ±2% for L40 and L62. In addition, there seems to be a bias in the current difference of E24-2 and L30-2 of approximately 1 A. The offset of EE current at the beginning of each measurement is always reset to zero, whereas this cannot be done with the BMS because there is no control over the measurement equipment. Perhaps the aforementioned biases can be attributed to such calibration issues. By comparing the SD in Table 5, it is visible that current differences are much more volatile than the voltage ones.

**Table 5.** Standard deviation and mean values of the percentage difference during constant current phase between EE and BMS datasets.

| | E24-1 | E24-2 | L30-1 | L30-2 | L40 | L62 |
|---|---|---|---|---|---|---|
| Voltage difference SD [%] | 0.05 | 0.04 | 0.04 | 0.03 | 0.03 | 0.01 |
| Voltage difference mean [%] | 0.11 | 0.21 | 0.22 | 0.27 | 0.1 | 0.03 |
| Current difference SD [%] | 3.46 | 2.82 | 3.43 | 1.35 | 0.35 | 0.28 |
| Current difference mean [%] | 1.92 | 3.79 | 1.26 | 4.96 | 0.39 | 1.39 |

Additionally, we should be reminded that the current measured with the EE also accounts for the DC/DC inverter losses present between the 400 V and 12 V buses, which can also be an explanation of the current differences. Furthermore, the unknown performance of the measurement equipment inside the EV is also expected to affect the accuracy of current values. However, given that the differences of voltage and current with the BMS and the EE are limited for most of the cars, in the next subsection capacity is estimated with the two datasets to determine the impact of the different measurements on capacity estimation.

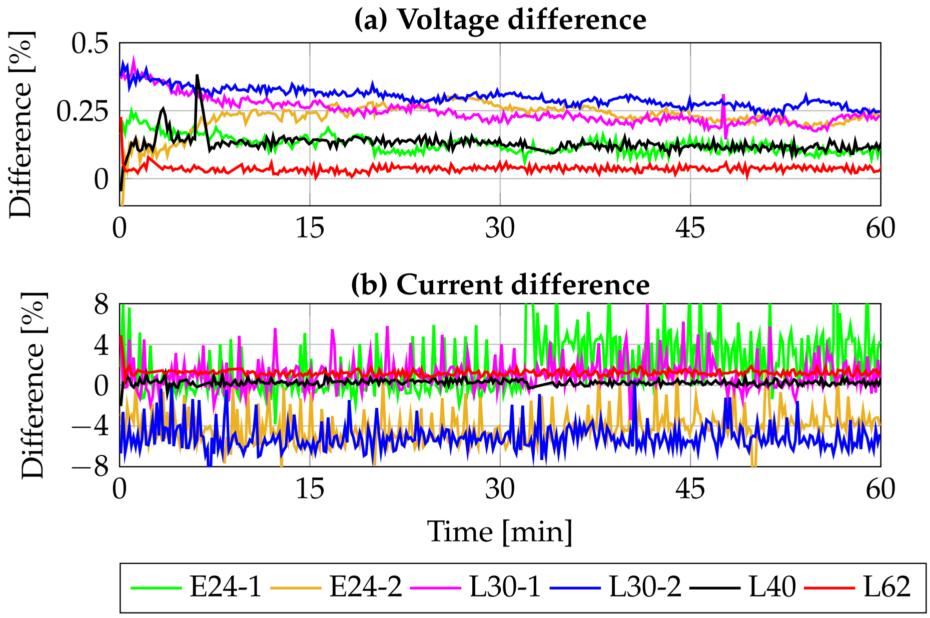


**Figure 7.** Comparison of voltage and current difference measured between EE and BMSs datasets. Subplot (**a**) shows the percentage voltage difference whereas (**b**) the percentage current difference.

### 5.3. Step 3: EE and BMS Capacity Estimation Comparison

The capacity estimated with the EE and BMS voltage and current datasets is reported in Table 6, in Ah and kWh. The difference between EE and BMS is limited to 3.8% for E24-2 and L30-2, and less than 1.5% for the remaining ones. This is in accordance with the findings from Figure 7b and Table 5, wherein currents for E24-2 and L30-2 prove to have an initial offset. Thus, the larger currents lead to a higher capacity estimation.

Thanks to the limited difference between the capacity estimated with the two datasets, it can be concluded that the BMS current and voltage values are accurate enough for estimating capacity with the ECE method. Because the BMS current and voltage data are directly collected at the battery terminals, this also means that the limitation of using DC chargers in the ECE method is lifted, and both chargers (AC and DC) can be used.

**Table 6.** Comparison of capacity derived with the ECE method with EE and BMS datasets in Ah and in kWh.

| | **Capacity in Ah** | | **Capacity in kWh** | |
|---|---|---|---|---|
| **Data** | **EE** | BMS | **EE** | **BMS** |
| E24-1 | 55.3 | 55.5 | 20.9 | 20.9 |
| E24-2 | 56.3 | 58.2 | 21.3 | 22.0 |
| L30-1 | 65.9 | 65.1 | 24.2 | 23.8 |
| L30-2 | 65.3 | 67.9 | 24.2 | 24.9 |
| L40 | 104.4 | 104.0 | 38.1 | 37.9 |
| L62 | 165.3 | 163.0 | 59.7 | 58.9 |
| | 164.4 | 162.5 | 59.6 | 58.9 |

### 5.4. Discussion

This section compares the findings, highlighting advantages and disadvantages of each estimation approach. The main results are summarized in Table 7.

**Table 7.** Data collection comparison.

| Characteristic/Data | EE | BMS | CAN-bus |
|---|---|---|---|
| **Measurement accuracy** | High | Medium/high, still unknown | Medium/high, still unknown |
| **Measurement location** | DC charger and 12 V bus | Battery terminals | Battery terminals |
| **Equipment** | Expensive | Limited (app to read data) | Limited (app to read data) |
| **Electrical knowledge** | Advanced | Limited | Limited |
| **Data processing info** | Full knowledge | Full knowledge | Limited knowledge |

The CAN-bus capacity readings cannot be fully interpreted by the authors, due to restricted knowledge on methodology and internal vehicle calculations. Therefore, this subsection mainly focuses on capacity measurements using EE and BMS current data, and insights regarding the quality and accessibility of the datasets is provided.

First, with the ECE method and EE measurements both a DC and an AC charger, current clamps, voltage differential probes, and a data logger are necessary. Such equipment with a reasonable accuracy is expensive and not readily available. In contrast, battery current is continuously measured by the BMS, but the accuracy of the measurements is unknown to the authors. The instantaneous difference between the current measured with EE and the BMS was found to be higher for older vehicles, and limited to 2% for the newest Nissan Leafs. In this comparison, it should be taken into account that EE measurements also include the DC/DC converter losses between the 400 V and the 12 V buses, which are instead bypassed with the BMS current measurement.

Secondly, DC chargers are used to bypass the AC/DC converter located between the AC charger and the 400 V bus. In addition to being more expensive, DC chargers have higher charging currents that result in higher joule losses during charging. By considering BMS data, current is directly measured at the battery terminals, meaning that both DC and AC chargers can be used. Given the observed limited difference between current readings from BMS and EE, it can be concluded that capacity estimation can be performed by using only onboard chargers and the BMS, without the need for expensive experimental setups.

Thirdly, to connect the external equipment to the 400 V side of the DC charger, it has to be possible to open the charger door and have access to the correct terminals, which also means that electrical component knowledge is required. On the other hand, BMS data is collected from the OBDII-CAN bus of the vehicle. For Nissan Leaf vehicles, information from the OBDII is made accessible by the Leaf Spy app, but similar applications could be developed for other cars.

The accessibility to BMS current measurements could greatly simplify ECE applicability by only using an OBDII, a mobile phone, and an AC charger. Thus, costs are decreased and collection time is limited, e.g., by charging the vehicle during night. Nevertheless, this comes with a need for BMS data reading and translation availability, which is at the moment accessible only for a few vehicles. A few commercial solutions are already using charging/discharging events to estimate battery capacity. These rely on data from the BMS, e.g., current, voltage, etc., to estimate the battery capacity. Because the full methodology is unknown to the user, our future research will compare the capacity estimations from these solutions with the methodology presented in this work.

## 6. Conclusions

The present paper investigated and compared capacity estimation approaches for six different EV batteries without disassembling them from the vehicles. The main objective of this work was to assess whether BMS readings can be used to circumvent the need for costly experimental measurements.

By connecting an OBDII to the vehicle CAN-bus, it is possible to read capacity estimates derived from the BMS. These were compared with the estimates from an empirical capacity method based on experimental measurements, showing large differences for older and smaller vehicles but acceptable deviations in newer and larger EVs. However, CAN-bus estimates are not transparent, they depend on the car manufacturer, and the underlying method may change over time, so no certain conclusions can be drawn regarding their use.

The empirical capacity estimation method, which consists of a full charge of the EV battery with a DC charger, was also used to estimate battery capacity. A DC charger is needed to bypass the AC/DC converter in the EV, and external measurement equipment is used to obtain reference capacity estimations independently of the ones reported by the BMS. However, with the OBDII connection it is also possible to collect current and voltage data directly measured at the battery terminals from the OBDII. This gives the possibility to estimate capacity with the empirical method by using the BMS current and voltage.

The instantaneous current and voltage measured from the BMS and the EE were compared, showing differences limited to $\pm 2\%$ for the newest vehicles and resulting in a capacity estimation difference of 1.5 percentage points. This confirms that BMS current values can be used to derive capacity, and that EV battery capacity tests can be greatly simplified by using an AC charger and an OBDII, without any electrical equipment know-how.

Future work should focus on the development of translation tools/apps to access and download BMS data. The tools/apps should be simple to understand and to apply, and should be compatible with as many EV brands and versions as possible. Finally, it is important to observe that the approaches presented in this paper are expected to be applicable to all car brands. However, complications in understanding the results can occur in the event that, for certain car models, the car releases battery capacity over the vehicle lifetime. This aspect will be further investigated in our future work.

**Author Contributions:** Conceptualization, L.C., C.Z., A.T., and M.M.; methodology, L.C., C.Z., and M.M.; validation, L.C.; formal analysis, L.C.; investigation, L.C.; data curation, L.C. and M.M; writing—original draft, L.C.; writing—review & editing, L.C., C.Z., A.T., and M.M.; visualization, L.C.; supervision, C.Z. and M.M.; funding acquisition, M.M.. All authors have read and agreed to the published version of the manuscript.

**Funding:** The work in this paper is supported by the research projects CAR (EU-Interreg grant nr: STHB.03.01.00-SE-S112/17) and ACDC (EUDP grant nr: 64019-0541).

**Institutional Review Board Statement:** Not applicable.

**Informed Consent Statement:** Not applicable.

**Data Availability Statement:** Data is not publicly available.

**Acknowledgments:** The icons used in Figure 1 were designed by Freepik from Flaticon.

**Conflicts of Interest:** The authors declare no conflict of interest. The funders had no role in the design of the study; in the collection, analyses, or interpretation of data; in the writing of the manuscript; or in the decision to publish the results.

## Abbreviations

The following abbreviations are used in this manuscript:

| | |
|---|---|
| MDPI | Multidisciplinary Digital Publishing Institute |
| FR | frequency regulation |
| SOC | state-of-charge |
| EV | electric vehicle |
| BMS | battery management system |
| SOH | state of health |
| V2G | vehicle-to-grid |
| ICA | incremental capacity analysis |
| NMC | nickel manganese cobalt |
| LMO | lithium manganese oxide |

OBDII on-board diagnostics port
IC incremental capacity
CAN central area network
OCV open circuit voltage
ECE empirical capacity estimation
SD standard deviation
EE external equipment

## Appendix A

### *Appendix A.1. BMS Data*

**Table A1.** Leaf Spy data (N/A stands for not available).

| | Vehicle Years | Distance [km] | $V_{in}$ [V] | $SOC_{in}$ [%] | $SOC_{end}$ [%] | $T_{in}$ [°C] | $T_{end}$ [°C] | $T_{out}$ [°C] |
|---|---|---|---|---|---|---|---|---|
| E24-1 | 2.6 | 9073 | 277 | 4.6 | 92.5 | 20 | 16 | N/A |
| | 3.5 | 14,380 | 282 | 8.9 | 91.8 | 35 | 15 | 5 |
| | 4.1 | 16,374 | 291 | 4.7 | 91.0 | 19 | 16 | 17 |
| | 4.5 | 17,061 | 296 | 7.5 | 90.3 | 20 | 16 | 19 |
| | 5.5 | 18,422 | 286 | 6.0 | 91.6 | 27 | 17 | N/A |
| E24-2 | 1.6 | 14064 | 275 | 5.6 | 94.2 | 16 | 21 | N/A |
| | 2.6 | 22,687 | 274 | 10.9 | 97.8 | 20 | 25 | 11 |
| | 3.1 | 24,724 | 308 | 4.9 | 94.0 | 19 | 24 | 14 |
| | 3.5 | 26,735 | 303 | 3.8 | 94.0 | 22 | 28 | 17 |
| | 4.0 | 30,999 | 307 | 9.4 | 94.1 | 13 | 19 | 10 |
| | 4.5 | 33,644 | N/A | 1.8 | 93.4 | 21 | 27 | 16 |
| L30-1 | 1.3 | 8147 | 266 | 3.2 | 97.7 | 26 | 25 | N/A |
| | 1.9 | 13,152 | 265 | 2.1 | 95.9 | 16 | 20 | N/A |
| | 2.3 | 17,058 | 258 | 2.4 | 97.6 | 22 | 24 | 12 |
| | 2.9 | 20,248 | 272 | 2.4 | 91.8 | 16 | 19 | 14 |
| | 3.2 | 22,999 | N/A | 0.7 | 97.7 | 21 | 22 | 18 |
| | 3.8 | 26,657 | 289 | 0.2 | 96.8 | 9 | 16 | 10 |
| | 4.2 | 30,719 | 286 | 0.0 | 97.8 | 25 | 28 | 16 |
| L30-2 | 2.1 | 17506 | 277 | 2.2 | 97.7 | 26 | 25 | N/A |
| | 2.7 | 21,676 | 285 | 3.4 | 96.5 | 19 | 21 | N/A |
| | 3.1 | 25,310 | 277 | 2.5 | 96.0 | 17 | 21 | 10 |
| | 3.7 | 28,202 | 264 | 3.2 | 97.7 | 14 | 20 | 13 |
| | 4.6 | 34,040 | 272 | 3.4 | 96.8 | 15 | 20 | 10 |
| | 5.1 | 38,524 | 297 | 0.6 | 97.8 | 23 | 27 | 16 |
| L40 | 1.1 | 35 | 271 | 0.9 | N/A | 37 | 32 | 23 |
| | 2.0 | 38 | 304 | 1.5 | 93.8 | 23 | 30 | 22 |
| | 2.9 | 43 | 294 | 0.1 | 93.9 | 24 | 32 | 23 |
| | 3.6 | 43 | 294 | 1.1 | 98.0 | 23 | 31 | 23 |
| | 3.8 | 43 | 283 | 1.2 | 98.0 | 24 | 31 | 23 |

**Table A1.** *Cont.*

| | Vehicle Years | Distance [km] | $V_{in}$ [V] | $SOC_{in}$ [%] | $SOC_{end}$ [%] | $T_{in}$ [°C] | $T_{end}$ [°C] | $T_{out}$ [°C] |
|---|---|---|---|---|---|---|---|---|
| L62 | 0.3 | 961 | 302 | 1.8 | 96.5 | 18 | 26 | 22 |
| | 1.0 | 12,631 | 290 | 1.8 | 96.9 | 26 | 30 | 22 |
| | 1.1 | 14,343 | 292 | 0.4 | 96.4 | 18 | 25 | 20 |

*Appendix A.2. Effect of AC Charger Tail*

DC chargers stop charging at approximately 3 A. If an AC charger is then connected, more energy can be stored in the battery. Consequently, a more accurate measurement of the actual capacity can be achieved by force-charging each vehicle in AC mode. Table A2 provides values for energy measured in A, B, and C, battery capacity, AC charging energy tail, and derived capacity, both with Ah and kWh.

The additional AC charged energy is limited, but not always negligible. For both E24 it represents 3–4% of the total capacity, with a minimum DC charging current of 3–4 A. This value was also observed for the E24 vehicles investigated in [14]. A lower value of 0.6% is measured for the L30-1, which is expected due to the low minimum current values reached with the DC charger of 1–2 A. L30-2 results are not provided because the DC charger stopped charging when the current was still constant at 24 A, due to equipment malfunction while conducting the experiment. For L40, the additional energy of 4% is caused by the considerable minimum DC charging current of 6 A. During the L62 measurements, the DC current reached 3 A, resulting in an additional energy of 0.7%. Given that the minimum current is typically 3 A, its influence on capacity is greater for smaller batteries, and for 62 kWh models it seems negligible. Results cannot be easily generalized though, because the minimum DC charging current also plays a role, and it seems to depend both on the DC charger and vehicle. Nevertheless, because it is still unclear why and when DC chargers stop charging, it is recommended to check the minimum DC current and consider the impact of the additional AC charging tail.

**Table A2.** Energy, battery capacity, and share of AC charging both considering Ah and kWh values.

| | Energy in A | Energy in B | Energy AC Charge (in C) | Battery Capacity | Share AC Charge |
|---|---|---|---|---|---|
| | | | **[Ah]** | | **[%]** |
| E24-1 | 55.1 | 2.0 | 2.2 | 55.3 | 4.0 |
| E24-2 | 56.2 | 1.9 | 2.0 | 56.3 | 3.5 |
| L30-1 | 66.6 | 1.1 | 0.4 | 65.9 | 0.6 |
| L40 | 101.9 | 1.8 | 4.3 | 104.4 | 4.0 |
| L62 | 167.1 | 2.9 | 1.1 | 165.3 | 0.7 |
| | 166.2 | 2.9 | 1.1 | 164.4 | 0.7 |
| | | | [kWh] | | [%] |
| E24-1 | 20.8 | 0.8 | 0.9 | 20.9 | 4.3 |
| E24-2 | 21.2 | 0.7 | 0.8 | 21.2 | 3.7 |
| L30-1 | 24.4 | 0.4 | 0.2 | 24.2 | 0.8 |
| L40 | 37.0 | 0.6 | 1.7 | 38.1 | 4.5 |
| L62 | 60.3 | 1.1 | 0.5 | 59.7 | 0.8 |
| | 60.2 | 1.0 | 0.4 | 59.6 | 0.7 |

## References


1. Waag, W.; Fleischer, C.; Sauer, D.U. Critical review of the methods for monitoring of lithium-ion batteries in electric and hybrid vehicles. *J. Power Sources* **2014**, *258*, 321–339. [CrossRef]
2. Stroe, D.I.; Schaltz, E. SOH Estimation of LMO/NMC-based Electric Vehicle Lithium-Ion Batteries Using the Incremental Capacity Analysis Technique. In Proceedings of the 2018 IEEE Energy Conversion Congress and Exposition, ECCE 2018, Portland, OR, USA, 23–27 September 2018; pp. 2720–2725. [CrossRef]
3. Hu, G.; Huang, P.; Bai, Z.; Wang, Q.; Qi, K. Comprehensively analysis the failure evolution and safety evaluation of automotive lithium ion battery. *eTransportation* **2021**, *10*, 100140. [CrossRef]
4. Berecibar, M.; Gandiaga, I.; Villarreal, I.; Omar, N.; Van Mierlo, J.; Van Den Bossche, P. Critical review of state of health estimation methods of Li-ion batteries for real applications. *Renew. Sustain. Energy Rev.* **2016**, *56*, 572–587. [CrossRef]
5. Gou, B.; Xu, Y.; Feng, X. State-of-Health Estimation and Remaining-Useful-Life Prediction for Lithium-Ion Battery Using a Hybrid Data-Driven Method. *IEEE Trans. Veh. Technol.* **2020**, *69*, 10854–10867. [CrossRef]
6. Xiong, R.; Tian, J.; Shen, W.; Sun, F. A Novel Fractional Order Model for State of Charge Estimation in Lithium Ion Batteries. *IEEE Trans. Veh. Technol.* **2019**, *68*, 4130–4139. [CrossRef]
7. Farmann, A.; Waag, W.; Marongiu, A.; Sauer, D.U. Critical review of on-board capacity estimation techniques for lithium-ion batteries in electric and hybrid electric vehicles. *J. Power Sources* **2015**, *281*, 114–130. [CrossRef]
8. Gong, X. Modeling of Lithium-ion Battery Considering Temperature and Aging Uncertainties. Ph.D. Thesis, University of Michigan-Dearborn, Dearborn, MI, USA, 2016.
9. Stroe, D.; Schaltz, E. Lithium-Ion Battery State-of-Health Estimation Using the Incremental Capacity Analysis Technique. *IEEE Trans. Ind. Appl.* **2020**, *56*, 678–685. [CrossRef]
10. Schaltz, E.; Stroe, D.I.; Nørregaard, K.; Stenhøj Kofod, L.; Christensen, A. Incremental Capacity Analysis for Electric Vehicle Battery State-of-Health Estimation. In Proceedings of the 2019 Fourteenth International Conference on Ecological Vehicles and Renewable Energies (EVER), Monte-Carlo, Monaco, 8–10 May 2019.
11. Schaltz, E.; Stroe, D.I.; Nørregaard, K.; Ingvardsen, L.S.; Christensen, A. Incremental Capacity Analysis Applied on Electric Vehicles for Battery State-of-Health Estimation. *IEEE Trans. Ind. Appl.* **2021**, *57*, 1810–1817. [CrossRef]
12. Tanim, T.R.; Shirk, M.G.; Bewley, R.L.; Dufek, E.J.; Liaw, B.Y. Fast charge implications: Pack and cell analysis and comparison. *J. Power Sources* **2018**, *381*, 56–65. [CrossRef]
13. Dubarry, M; Beck, D.; Perspective on Mechanistic Modeling of Li-Ion Batteries. *Accounts Mater. Res.* **2022**, *3*, 843–853. https://10.1021/accountsmr.2c00082. [CrossRef]
14. Thingvad, A.; Calearo, L.; Andersen, P.B.; Marinelli, M. Empirical Capacity Measurements of Electric Vehicles Subject to Battery Degradation from V2G Services. *IEEE Trans. Veh. Technol.* **2021**, *70*, 7547–7557. [CrossRef]
15. Calearo, L.; Thingvad, A.; Ziras, C.; Marinelli, M. A methodology to model and validate electro-thermal-aging dynamics of electric vehicle battery packs. *J. Energy Storage* **2022**, *55*, 105538. [CrossRef]
16. Meng, J.; Cai, L.; Stroe, D.I.; Luo, G.; Sui, X.; Teodorescu, R. Lithium-ion battery state-of-health estimation in electric vehicle using optimized partial charging voltage profiles. *Energy* **2019**, *185*, 1054–1062. [CrossRef]
17. EN IEC 62660-1:2019(MAIN) Secondary Lithium-Ion Cells for the Propulsion of Electric Road Vehicles—Part 1: Performance Testing. Available online: https://standards.iteh.ai/catalog/standards/clc/8ea64757-cca6-4dff-b2f9-af5997976f3c/en-iec-62660-1-2019 (accessed on 1 June 2022).
18. Pollock, J. *LeafSpy Help Version 1.50, User Manual*; LeafSpy Pro: Cupertino, CA, USA, 2022.
19. Electric Vehicle Lithium-Ion Battery. Available online: https://www.nissan-global.com/EN/TECHNOLOGY/OVERVIEW/li_ion_ev.html (accessed on 20 October 2021).
20. Marinelli, M.; Thingvad, A.; Calearo, L. *Across Continents Electric Vehicles Services Project: Final Report*; Technical University of Denmark: Lyngby, Denmark, 2020.
21. Marinelli, M.; Calearo, L.; Engelhardt, J.; Rohde, G. Electrical Thermal and Degradation Measurements of the LEAF e-plus 62-kWh Battery Pack. In Proceedings of the 2022 International Conference on Renewable Energies and Smart Technologies IEEE, Tirana, Albania, 28–29 July 2022.
22. Calearo, L.; Marinelli, M.; Ziras, C. A review of data sources for electric vehicle integration studies. *Renew. Sustain. Energy Rev.* **2021**, *151*, 111518. [CrossRef]